European Journal of Radiology 110 (2019) 45–53

Contents lists available at ScienceDirect

European Journal of Radiology

journal homepage: www.elsevier.com/locate/ejrad

Research article

Meningioma grading using conventional MRI histogram analysis based on 3D tumor measurement

Xiaoxin Li[a], Yanwei Miao[a,*], Liang Han[a], Junyi Dong[a], Yan Guo[b], Yuqing Shang[c], Lizhi Xie[d], Qingwei Song[a], Ailian Liu[a]

[a] Department of Radiology, the First Affiliated Hospital of Dalian Medical University, Dalian, Liaoning, China
[b] Life Science, GE Healthcare, Shenyang, Liaoning, China
[c] Department of Chronic Disease Epidemiology, Yale School of Public Health, Yale University, New Haven, Connecticut, USA
[d] GE Healthcare, MR Research China, Beijing, China

ARTICLE INFO

Keywords:
Meningiomas
Magnetic resonance imaging
Histogram
Grade

ABSTRACT

Purpose: To evaluate the application of conventional MRI histogram analysis based on the whole tumor measurement on assessing meningioma grading.

Materials and Methods: This retrospective study was approved by the institutional review board. A total amount of 90 patients with meningioma were enrolled and the preoperative MRI of them were analyzed. To be specific, the patient group were consisted of 45 patients with grade I, 38 with grade II, and 7 with grade III meningioma. Grade I meningioma is classified as low grade meningioma (LGM), whereas Grade II and III meningioma were combined and classified as high grade meningioma (HGM). ROIs were drawn along the edge of the tumor on each section of T1WI, T2WI, and contrasted T1WI. 3D ROI signal intensity histogram and all its parameters were obtained. Independent *t*-test and Kruskal-Wallis test were used for comparison between two groups. Univariate logistic regression analysis and Spearman's correlation analysis were used to screen for the parameters with high predictive efficiency, while multivariate logistic regression analysis was used to determine the optimal model for the classification of meningioma.

Results: There were significant differences observed between HGM and LGM groups regarding to histogram volume count, uniformity of three sequences, range of T1WI and T2WI, kurtosis, standard deviation, variance, max intensity of T2WI, skewness, mean deviation, minimum intensity, mean value, the 5th percentile, the 10th percentile, the 25th percentile, the 50th percentile, the 75th percentile, and the 90th percentile of contrasted T1WI. Volume count and uniformity were high predictive parameters in distinguishing HGM from LGM. Logistic regression model included contrasted T1WI histogram parameters (i.e. minimum intensity, volume count, skewness, uniformity, and the 75th percentile) showed the best diagnostic efficiency for meningioma grade, with a sensitivity and specificity of 83.9% and 77.4% (AUC = 0.834, cutoff value = 0.413), respectively. The optimal model was achieved with a sensitivity of 71.4% and a specificity of 78.6% in the test set (AUC = 0.791, cutoff value = 0.413).

Conclusions: Histogram analysis of conventional MRI based on 3D tumor measurement can be applied in the assessment of meningioma grading in clinical.

1. Introduction

Meningiomas are common extra-axial neoplasms that are classified into three grades, including typical (grade I), atypical (grade II), and malignant (grade III) ones [1]. Approximately, 90% of meningiomas are typical, whereas the remaining 10% consist of atypical and malignant ones. Atypical or malignant meningiomas have high mortality and recurrence rates due to their aggressive behaviors, thus, meningioma grading is of extreme significance for prognosis and the determination of treatment plan [2–4]. Tumor grading is characterized by the heterogeneity resulted from wide range of genotypes and phenotypes [5,6].

MRI demonstrates water composition within living organs and tissues that contributes to predicting the pathological information of the corresponding body parts. Conventional MRI signal intensity has been used to detect the heterogeneity and histopathological subtypes of the tumor in meningioma, whereas its reliability on tumor grading was not fully confirmed or even convincing [7]. One conclusion marked by Yao A et al in a systematic review was that T2WI signal intensity provided a useful

* Corresponding author.
E-mail address: ywmiao716@163.com (Y. Miao).

https://doi.org/10.1016/j.ejrad.2018.11.016
Received 10 August 2018; Received in revised form 4 November 2018; Accepted 18 November 2018

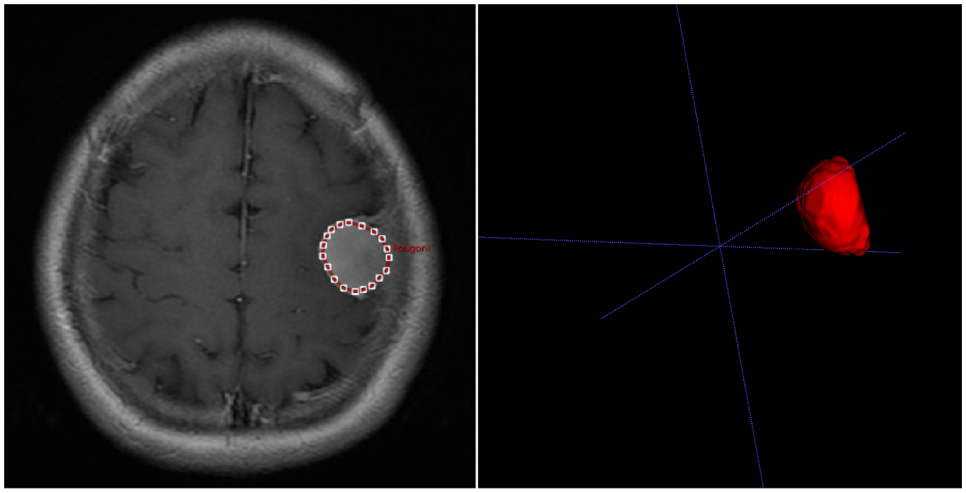

A B

Fig. 1. Image A shows ROIs were drawn along the edge of tumor parenchyma. Image B is a composite of multiple A, that is to say, B represents a three-dimensional structure of tumor.

predictive measurement of tumor consistency, whereas T1WI was not found to offer any diagnostic or predictive value [8]. The unsatisfied predictive ability for tumor grading has been hypothesized by the limitation of using naked eyes and local ROI selection during signal intensity analysis. Using naked eyes to analyze signals restricted the objectivity and accuracy for measurements and is subjective to potential bias. In addition, the most applied tumor select method is to select 2–3 small ROIs in tumor parenchyma or edema region, while avoiding hemorrhage, necrosis and cystic changes. However, this approach is not comprehensive and cannot fully or accurately reflect the heterogeneity of tumor, not to mention the possibility of individual selection bias and sampling error [9,10]. Yusuhn Kang et al found that a placement of ROIs covering the entire volume of tumor would eliminate the potential sampling bias, providing more objective and quantitative information on tissue characteristics and heterogeneity of whole tumor [9,11–13]. On the basis of global analysis in brain tumors, histogram can provide more abundant information on tumor heterogeneity, comparing to mean value or standard deviation [14]. Tumor areas with different T1WI, T2WI or contrasted T1WI characteristics can be reflected on the histogram, that is to say, all elements contributing to the tumor grading will be compared side by side. Recently, histogram analysis of conventional or advanced MRI technology has been successfully applied to brain tumor grading or differential diagnosis [9,15–25]. However, to the best of our knowledge, conventional MRI histogram analysis, including T1WI, T2WI and contrasted T1WI,is rarely reported for meningioma grading, while only two studies demonstrated the application of contrasted T1WI in meningioma grading. T1WI and T2WI histogram analysis have not been reported yet [26,27].

Therefore, the purpose of the current study is to explore the application of histogram analysis of conventional MRI based on 3D tumor measurement in meningioma grading.

2. Materials and methods

2.1. Patient selection

The current study was approved by the institutional review board. The preoperative MRI were performed on 45 patients with grade I meningiomas (11 males and 34 females; mean age: 53.7 ± 11.1 years), 38 with grade II meningiomas (19 males and 18 females; mean age: 61.4 ± 9.7 years), and 7 with grade III meningiomas (3 males and 4 females; mean age: 64.0 ± 11.3 years) at our institution from January 2010 to December 2016. Their MRI results were retrospectively analyzed. Grade II and III meningiomas were combined into one group as high grade meningioma (HGM) whereas Grade I meningioma was classified as low grade meningioma (LGM) for analysis. Histopathologic classification of tumor was performed according to the World Health Organization criteria, with the exclusion of images with artifacts.

2.2. Data acquisition

MRI acquisitions were performed on a 3.0 T whole-body unit (Signa HDxt, General Electric Co., Milwaukee, WI, USA) with an eight-channel phased-array head coil. MRI sequences included axial T1WI and contrasted T1WI spin-echo with the following parameters: TR/TE = 400 ms/9.0 ms; FOV: 220 mm × 220 mm; matrix: 448 × 256; section thickness: 6 mm; intersection gap: 1 mm, and axial T2WI fast spin-echo (TR/TE = 4000 ms/110 ms; FOV: 220 mm × 220 mm; matrix: 448 × 256; section thickness: 6 mm; intersection gap: 1 mm).

2.3. Image processing

Axial T1WI, T2WI, and contrasted T1WI images were imported into Omni-Kinetics software, where ROIs containing tumor parenchyma were manually depicted along the edge of tumor on each layer of image, the ROIs of all layers were merged into a 3D ROI (Fig. 1). For tumors with a clear boundary clear, the ROI is easy to determine, meanwhile, there are remaining high-level meningiomas whose boundary is obscure. Contrasted T1WI is particularly important in determining tumor ROI, which is capable to provide. an easier-to-sketch boundary between meningioma and the surrounding organization structure. We took reference of contrasted T1WI ROI while determining the ROI on T1WI and T2WI, in order to achieve consistent results with the contrasted T1WI ROI. Then, 3D ROI signal intensity histograms of T1WI, T2WI, and contrasted T1WI were automatically obtained, along with all the parameters listed as follows: min intensity, max

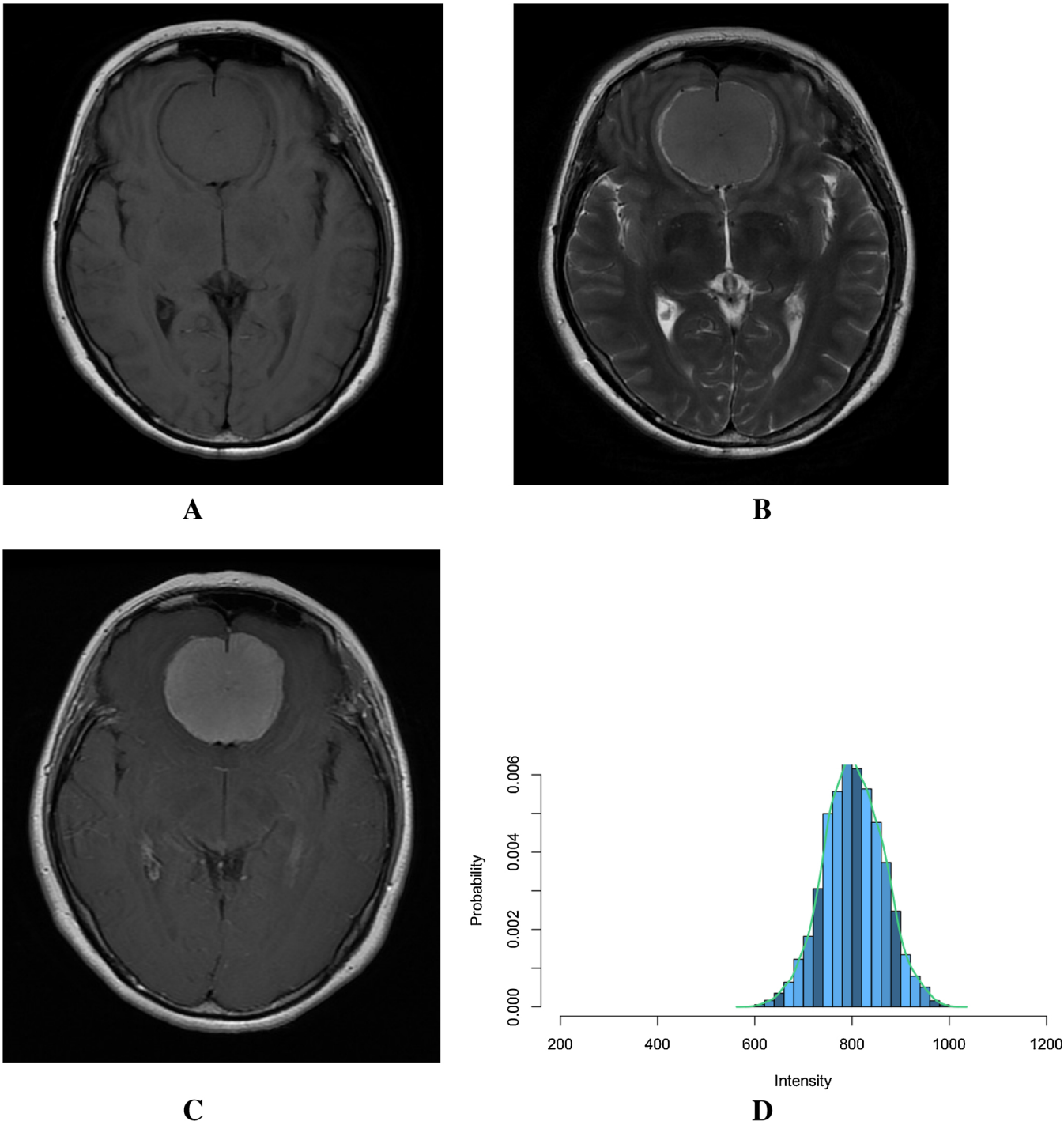

Fig. 2. Image A–F are T1WI, T2WI, contrasted T1WI, and their respective histograms of LGM. Tumor is isointensity on both T1WI(A) and T2WI(B), there is significantly homogeneous enhancement on contrasted T1WI(C). Histogram fitting curves of LGM are high and sharp. Image G–L are T1WI, T2WI, contrasted T1WI and their respective histograms of HGM. Tumor is iso- or hypointensity on T1WI(G), and iso- or hyperintensity on T2WI(H). Tumor shows homogeneous enhancement on contrasted T1WI(I). The histogram fitting curves of HGM are wide and flat compared to LGM, and the morphology of histogram is unstable (i.e. a partial or a double peak). The MRI manifestations of HGM and LGM are similar, but the histogram are different. Therefore, histogram conduces to meningioma classification.

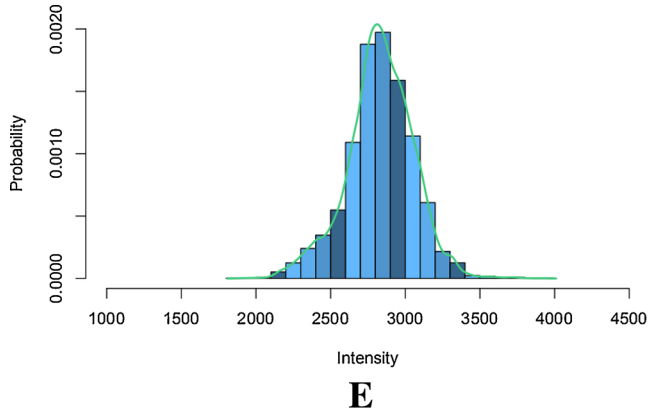

E

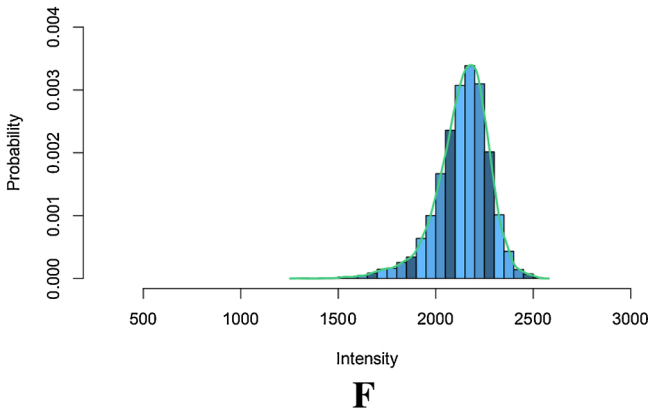

F

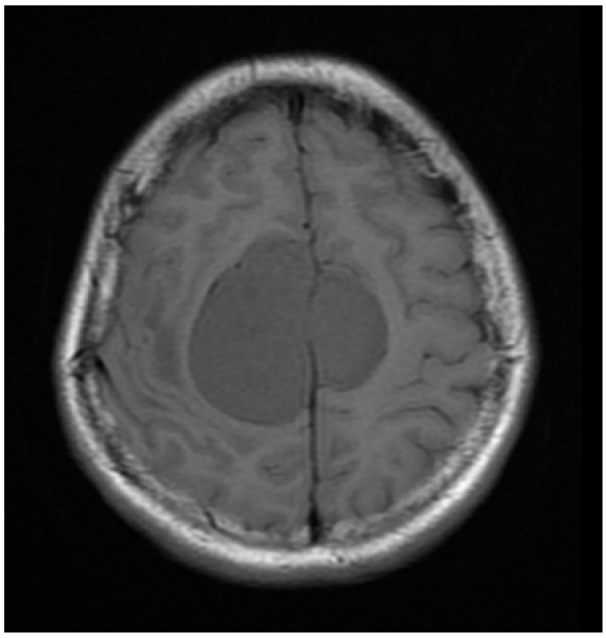

G

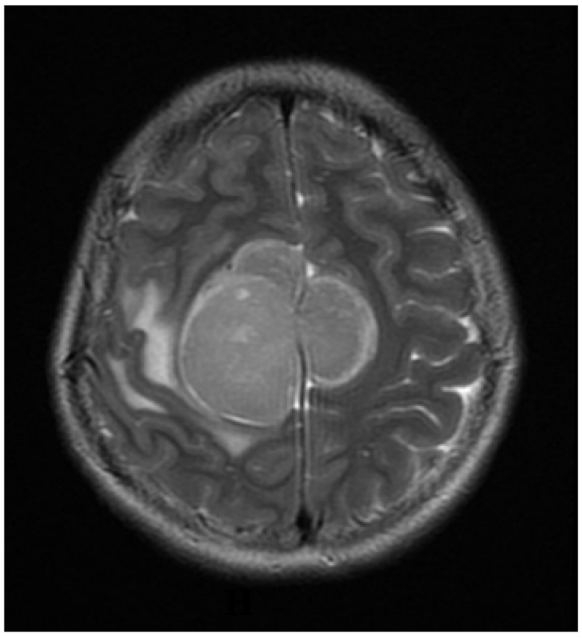

H

Fig. 2. (*continued*)

intensity, mean value, range, volume count, standard deviation, variance, mean deviation, skewness, kurtosis, uniformity, the 5^{th}, 10^{th}, 25^{th}, 50^{th}, 75^{th}, 90^{th}, and 95^{th} percentiles.

2.4. Statistical analysis

All statistical analyses were conducted using R language software. Intraclass correlation coefficient (ICC) test was performed to test the consistency of histogram parameters that were delineated by two independent radiologists prior to data analysis. The comparison between two groups would be performed if ICC test returned a consistent results (i.e. ICC ≥ 0.75). Independent-samples *t*-test and Kruskal-Wallis test were used for comparison, with P value < 0.05 considered as statistically significant. Univariate logistic regression analysis (P < 0.05) and Spearman's correlation analysis (P ≥ 0.05 or P < 0.05, r < 0.9) were used to screen for the parameters with high predictive power. Parameters with high predictive power were fed into a multivariate logistic regression analysis to determine an optimal logistic regression model for tumor classification. 31 cases in each group was considered as training set, which was used to establish the logistic regression model. On the other hand, the remaining 14 cases in each group were test set, which was applied to detect model accuracy. All the parameters with high predictive power were integrated into one variable, and ROC curve was constructed to assess the grading ability of logistic regression model.

3. Results

Representative images and histograms from meningioma patients are demonstrated in Fig. 2. Both histogram volume count and uniformity changed with the increase of tumor grade on T1WI, T2WI and contrasted T1WI images. Particularly, volume variation increased with tumor grade, whereas uniformity showed the tendency to decrease. It is noticeable that

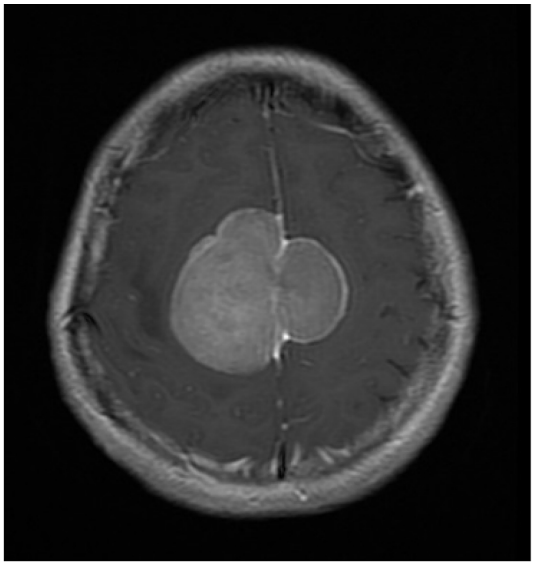

I

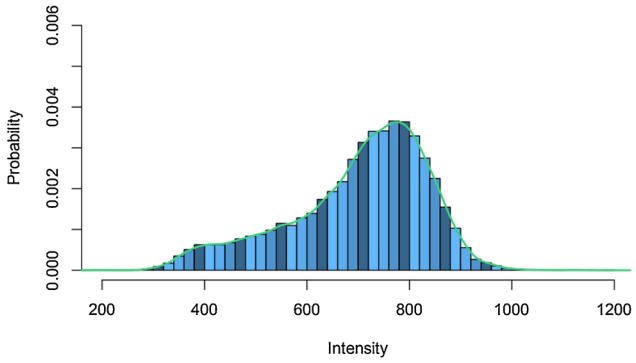

J

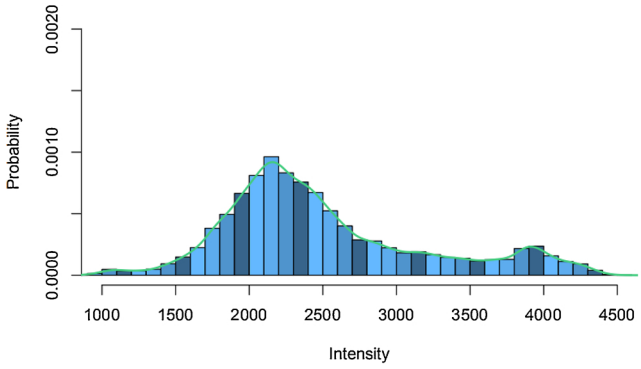

K

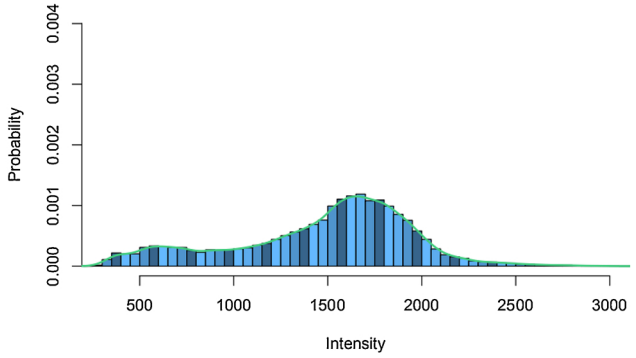

L

Fig. 2. (*continued*)

the inconsistent volume count measured on T1WI, T2WI and contrasted T1WI in Fig. 2 was due to an error while drawing the ROIs. Moreover, a comparison was conducted to prove the difference among those three was not statistically significant ($P > 0.05$). Range differed significantly between two groups on T1WI and T2WI images. Standard deviation and variance were significantly different between two groups on T2WI, while HGM were distinctly greater than those of LGM. A significant difference was observed between grades for min intensity, mean value, the 5^{th}, 10^{th}, 25^{th}, 50^{th}, 75^{th}, and 90^{th} percentiles in contrasted T1WI, where all of these parameters were higher in LGM than HGM. Max intensity, kurtosis of T2WI histogram and skewness, mean deviation of contrasted T1WI histogram were proved to be significant histogram parameters for distinguishing high- from low-grade meningioma. Other histogram parameters did not show significant inter-group differences. Histogram parameters with significant differences between grades are demonstrated in Table 1.

Univariate logistic regression analysis and Spearman's correlation analysis selected 2 out of 3 parameters on T1W1, 4 out of 7 on T2W1, and 5 out of 12 on contrasted T1WI respectively, which had high predictive power to establish models. Correlation coefficient matrix heat maps of histogram parameters with high predictive power are shown in Fig. 3, taking T2WI histogram parameters as an example. ROC curve maps are shown in Fig. 4.

Thereafter, the optimal logistic regression models of T1WI, T2WI and contrasted T1WI were determined for T1W1, T2W1, and contracted T1W1 as follows:

$$f_{(T1WI)} = 9.54 + 5.29e^{-5} \times \text{VolumeCount-}12.1 \times \text{Uniformity}$$

$$f_{(T2WI)} = 6.41 + 3.59e^{-5} \times \text{VolumeCount} + 2.68e^{-5} \times \text{Range-}0.17 \times \text{Kurtosis}^{-7}.84 \times \text{Uniformity}$$

$$f_{(\text{contrasted T1WI})} = 6.08 + 7.64e^{-4} \times \text{MinIntensity} + 4.24e^{-5} \times \text{VolumeCount} + 0.84 \times \text{Skewness-}6.23 \times \text{Uniformity-}1.10e^{-3} \times 75^{th}$$

ROC curve showed that the optimal model for meningioma grading included contrasted T1WI histogram parameters with high predictive power, which had a cutoff value of 0.413, a sensitivity of 83.9%, a

Table 1
Histogram parameters of LGM and HGM.

Parameters	LGM	HGM	P value
T1WI			
Volume count	8613.00 ± 15,074.50	9157.54 ± 9924.05	< 0.01
Range	506.00 ± 442.00	25843.00 ± 36,549.00	0.04
Uniformity	0.90 ± 0.07	0.87 ± 0.04	0.02
T2WI			
Volume count	8470.00 ± 14,171.5	25533.00 ± 51,505.00	< 0.01
Range	1361.00 ± 2795.5	2186.00 ± 3262.5	0.01
Uniformity	0.85 ± 0.06*	0.79 ± 0.06*	< 0.01
Max-intensity	360.00 ± 387.00	231.00 ± 429.00	0.03
Standard deviation	177.21 ± 219.25	279.23 ± 372.49	< 0.01
Variance	31402.80 ± 82,469.94	77968.70 ± 237,250.95	< 0.01
Kurtosis	5.34 ± 3.89	4.31 ± 2.87	< 0.01
Contrasted T1WI			
Volume count	7383.00 ± 15,481.5	25545.00 ± 40,447.5	< 0.01
Uniformity	0.86 ± 0.06	0.82 ± 0.07	< 0.01
Min-intensity	399.00 ± 425.5	327.00 ± 323.00	0.04
Mean value	1749.29 ± 1042.5	1362.18 ± 840.84	0.01
Mean deviation	−1494.77 ± 1042.54	−1107.72 ± 841.07	0.01
Skewness	−0.86 ± 0.61*	−0.33 ± 0.56*	< 0.01
5th percentile	1240.34 ± 672.78	796.78 ± 648.33	< 0.01
10th percentile	1409.54 ± 745.32	939.88 ± 756.20	< 0.01
25th percentile	1539.97 ± 944.91	1165.87 ± 855.75	< 0.01
50th percentile	1739.14 ± 1057.83	1359.29 ± 853.21	0.01
75th percentile	1907.05 ± 1126.97	1521.02 ± 866.81	0.02
90th percentile	2006.93 ± 1176.11	1704.13 ± 975.93	0.04

Note: Unless particularly stated as means ± SD(*), data shown are median ± interquartile. Unless stated as Independent-samples *t*-test(*), differences between LGM and HGM were evaluated using Kruskal-Wallis test.

specificity of 77.4%, and AUC of 0.834. These logistic regression models were revealed by the test set under the circumstances that 79.1% (T1WI), 78.1% (T2WI), and 82.1% (contrasted T1WI) of cases were correctly classified using the respective model.

4. Discussion

The results of our study suggested that histogram volume count and uniformity were equipped with highly differential efficiency between HGM and LGM on three sequences, thus we believe that they are more persuasive parameters for tumor grading. Logistic regression model derived from contrasted T1WI histogram parameters showed better diagnostic performance than the other two sequences, reflecting that contrasted T1WI is more reliable for the identification of HGM and LGM. Previous studies showed that histogram analysis of advanced MRI parameters has been successfully applied to brain tumor grading [9,15–17,24]. Yusuhn Kang's study of histogram analysis of ADC maps for grading gliomas using the same method of our study, that is 3D tumor measurement [9]. A study by Wang Sumei et al showed that the histogram analysis of DTI parameters could contribute to the determination of meningioma grades [15]. However, the purpose of our study was to explore the diagnostic value of conventional MRI sequences (i.e. T1WI, T2WI and contrasted T1WI) but not functional sequences. The reason was that T1WI, T2WI and contrasted T1WI represent the most common approach of meningioma pretherapeutic diagnostics, especially in primary care health facilities and hospitals, where advanced MRI technologies have not been introduced yet. Although Thibaud P. Coroller and Georg Alexander Gihr have both proved the contribution of contrasted T1WI histogram analysis on meningioma histopathologic grading, whereas the clinical value of T1WI and T2WI were not mentioned [26,27]. Therefore, the novelty of this paper lies in expounding comprehensively diagnostic value of T1WI, T2WI and contrasted T1WI histogram analysis. In addition, Qi XX et al found that DKI histogram analysis would effectively differentiate low- from high-grade gliomas, especially mean MK, which was the best independent predictor of glioma grading [16]. It was proven that histogram parameters from ktrans(DCE) and rCBF(DSC) could efficiently discriminate gliomas grades [17,24]. All of the above previous studies certainly imply that histogram analysis provides a more comprehensive and sensitive assessment on detecting tumor heterogeneity. Thus, The prospect of histogram analysis to classify tumor is considerable as well.

HGM is characterized by the loss of normal tissue or cell structure and focal necrosis, and these features result greater heterogeneity in HGM comparing to that of LGM. Histogram range and uniformity are important indexes to reflect the change of image intensity in tumors. In the current study, HGM were observed with higher heterogeneity due to larger range and lower uniformity compared to LGM. This is in concordance with the results showing significantly higher variance and standard deviation of T2WI histogram in HGM. The presence of internal cystic degeneration, necrosis, and hemorrhage in HGM may be attributable to heterogeneity enhancement [10–12,25]. Volume count gradually increased with the increase of tumor grade, which may represent rapid growth or aggressive behaviors of tumor cells [28–30]. Skewness and kurtosis describe the distribution of histogram curves, which are excellent indicators of tumor heterogeneity. Moreover, these two parameters are often correlated with the malignancy degree of tumor, thus, they can be used as independent factors to evaluate prognosis [18]. A previous study has revealed higher kurtosis and skewness in atypical or malignant meningiomas compared to that in typical meningiomas. However, our results showed contradictory results with the previous study [15] by observing higher kurtosis and skewness in LGM. The discrepancy may be resulted from angiomatous meningioma, which is a subtype of grade I meningiomas but resembles high-grade aggressive meningiomas [31,32]. In the previous study, there were only two angiomatous meningiomas included, whereas, nine cases were present in our study. This might be the same reason of observing a higher value of contrasted T1WI histogram parameters (i.e. min intensity, mean value, 5^{th}, 10^{th}, 25^{th}, 50^{th}, 75^{th}, and 90^{th} percentile) in grade I meningiomas. Meningiomas are observed with significantly enhancement on contrasted T1WI due to abundant blood supply, especially in angiomatous meningiomas, which are characterized by blood vessels occupying more than 50% of the tumor volume. Since the blood supply of angiomatous meningioma exceeds HGM [33], this could explain overall elevated contrasted T1WI signal. Therefore, further studies with more angiomatous meningioma cases are required to address this issue.

According to logistic regressions model and ROC curve analysis, contrasted T1WI shows the best diagnostic grading performance compared to the remaining two sequences. Thus, contrasted T1WI histogram parameters may be the most reliable method for accessing meningioma grades.

Apart from the intrinsic limits of any retrospective study, another limitation of our study is the restricted number of grade III meningiomas and subtypes, accordingly, a differential diagnosis between grade II and III meningiomas and a diagnosis among meningioma subtypes were absent.

In conclusion, histogram analysis of conventional MRI based on 3D tumor measurement can be a useful diagnostic tool for grading meningiomas, especially using volume count and uniformity as predicators. The logistic regression model obtained from contrasted T1WI histogram parameters is the most promising assessment for meningioma grading.

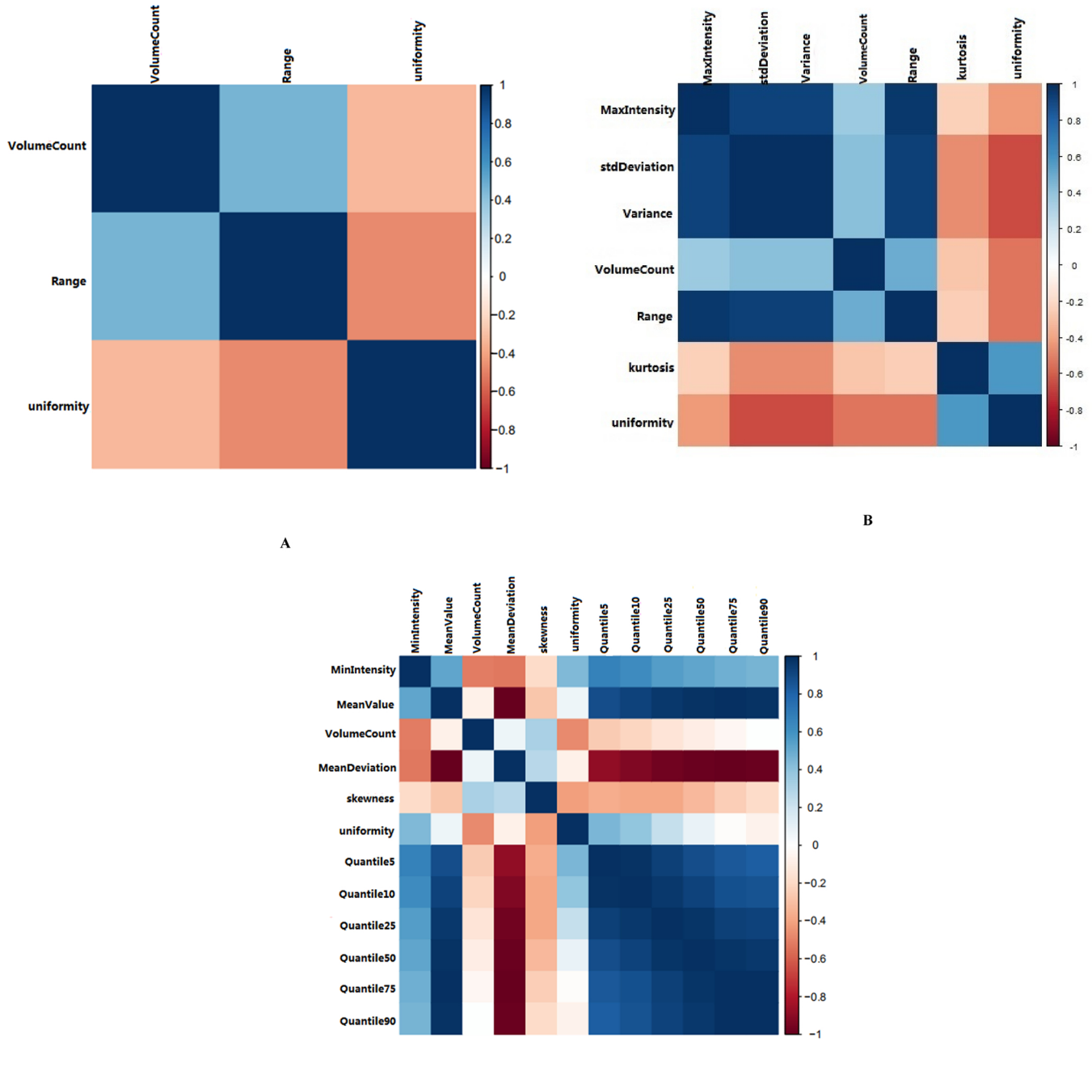

Fig. 3. Correlation coefficient matrix heat map of T1WI (A), T2WI (B), contrasted T1WI (C) histogram parameters with statistically significant difference. The darker color indicates a stronger correlation between parameters, where blue represents positive correlation and red represents negative correlation. Take T2WI (B) for example, lighter colors (i.e. weaker correlation) were observed for volume count, range, kurtosis, uniformity than other parameters, thus, these four parameters were selected to establish the models of T2WI.

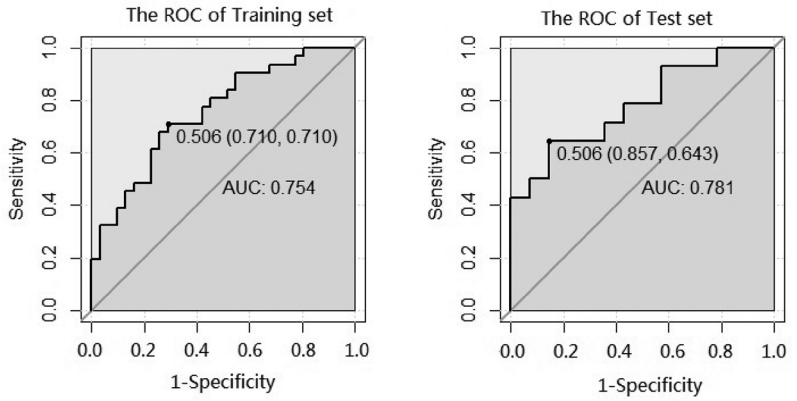

A

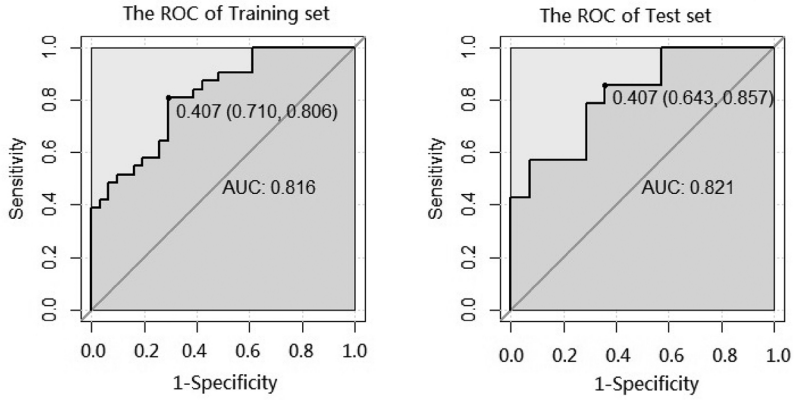

B

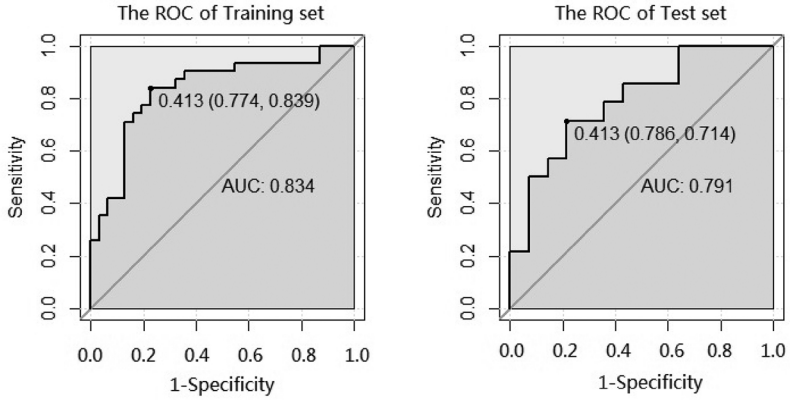

C

Fig. 4. Image A, B, and C showed the ROC curves for evaluating the models established by T1WI, T2WI, and contrasted T1WI histogram parameters with high predictive efficiency screened by univariate logistic regression analysis and Spearman's correlation analysis. The model of contrasted T1WI is equipped with the best diagnostic efficiency, with a sensitivity of 83.9%, specificity of 77.4%, and AUC of 0.834. It was revealed by the test set that 79.1% of cases were correctly classified using the contrasted T1WI model.

Conflictsof interest

The authors have no conflicts of interest to declare.

Acknowledgement

National Natural Science Foundation (81671646).

References

[1] D.N. Louis, A. Perry, G. Reifenberger, et al., The 2016 world health organization classification of tumors of the central nervous system: a summary, Acta Neuropathol. 131 (6) (2016) 803–820.
[2] P. Zhao, M. Hu, M. Zhao, et al., Prognostic factors for patients with atypical or malignant meningiomas treated at a single center, Neurosurg. Rev. 38 (1) (2015) 101–107 discussion 107.
[3] G. Kaur, E.T. Sayegh, A. Larson, et al., Adjuvant radiotherapy for atypical and malignant meningiomas: a systematic review, Neuro Oncol. 16 (5) (2014) 628–636.
[4] A. Nowak, T. Dziedzic, P. Krych, Benign versus atypical meningiomas: risk factors predicting recurrence, Neurol. Neurochir. Pol. 49 (1) (2015) 1–10.
[5] L. Alic, W.J. Niessen, J.F. Veenland, Quantification of heterogeneity as a biomarker in tumor imaging: a systematic review, PLoS One 9 (10) (2014) e110300.
[6] L.S. Hu, S. Ning, J.M. Eschbacher, et al., Multi-parametric MRI and texture analysis to visualize spatial histologic heterogeneity and tumor extent in Glioblastoma, PLoS One 10 (11) (2015) e0141506.
[7] Benita Tamrazi, Mark S. Shiroishi, Chia-Shang J. Liu, Advanced imaging of intracranial meningiomas, Neurosurg. Clin. N. Am. 27 (2) (2016) 137–143.
[8] A. Yao, M. Pain, P. Balchandani, et al., Can MRI predict meningioma consistency?: a correlation with tumorpathology and systematic review, Neurosurg. Rev. 41 (3) (2018) 745–753.
[9] Y. Kang, S.H. Choi, Y.J. Kim, Gliomas: histogram analysis of apparent diffusion coefficient maps with standard- or high-b-value diffusion-weighted MR imaging–correlation with tumor grade, Radiology 261 (3) (2011) 882–890.
[10] N. Just, Improving tumour heterogeneity MRI assessment with histograms, Br. J. Cancer 111 (12) (2014) 2205–2213.
[11] S.J. Ahn, S.H. Choi, Y.J. Kim, et al., Histogram analysis of apparent diffusion coefficient map of standard and high B-value diffusion MR imaging in head and neck squamous cell carcinoma: a correlation study with histological grade, Acad. Radiol. 19 (10) (2012) 1233–1240.
[12] Y.J. Ryu, S.H. Choi, S.J. Park, et al., Glioma: application of whole-tumor texture analysis of diffusion-weighted imaging for the evaluation of tumor heterogeneity, PLoS One 9 (9) (2014) e108335.
[13] Y.D. Zhang, Q. Wang, C.J. Wu, et al., The histogram analysis of diffusion-weighted intravoxel incoherent motion (IVIM) imaging for differentiating the gleason grade of prostate cancer, Eur. Radiol. 25 (4) (2015) 994.
[14] A.L. Krivoshapkin, G.S. Sergeev, L.E. Kalneus, et al., New software for preoperative diagnostics of meningeal tumor histologic types, World Neurosurg. 90 (2016) 123–132.
[15] S. Wang, S. Kim, Y. Zhang, et al., Determination of grade and subtype of meningiomas by using histogram analysis of diffusion-tensor imaging metrics, Radiology 262 (2) (2012) 584–592.
[16] X.X. Qi, D.F. Shi, S.X. Ren, et al., Histogram analysis of diffusion kurtosis imaging derived maps may distinguish between low and high grade gliomas before surgery, Eur. Radiol. 28 (4) (2018) 1748–1755.
[17] A. Falk, M. Fahlström, E. Rostrup, et al., Discrimination between glioma grades II and III in suspected low-grade gliomas using dynamic contrast-enhanced and dynamic susceptibility contrast perfusion MR imaging: a histogram analysis approach, Neuroradiology 56 (12) (2014) 1031–1038.
[18] H.J. Baek, H.S. Kim, N. Kim, et al., Percent change of perfusion skewness and kurtosis: a potential imaging biomarker for early treatment response in patients with newly diagnosed glioblastomas, Radiology 264 (3) (2012).
[19] Shin-Lei Penga, Chih-Feng Chenb, Ho-Ling Liu, et al., Analysis of parametric histogram from dynamic contrast-enhanced MRI: application in evaluating brain tumor response to radiotherapy, NMR Biomed. 26 (2013) 443–450.
[20] V. Nardone, P. Tini, M. Biondi, et al., Prognostic value of MR imaging texture analysis in brain Non-SmallCell lung Cancer oligo-Metastases undergoing stereotactic irradiation, Cureus 8 (4) (2016) e584.
[21] N. Michoux, A. Guillet, D. Rommel, et al., Texture analysis of T2-Weighted MR images to assess acute inflammation in brain MS lesions, PLoS One 10 (12) (2015) e0145497.
[22] L.S. Hu, S. Ning, J.M. Eschbacher, et al., Multi-parametric MRI and texture analysis to visualize spatial histologic heterogeneity and tumor extent in Glioblastoma, PLoS One 10 (11) (2015) e0141506.
[23] K. Murayama, Y. Nishiyama, Y. Hirose, et al., Differentiating between central nervous system lymphoma and high-grade glioma using dynamic susceptibility contrast and dynamic contrast-enhanced MR imaging with histogram analysis, Magn. Reson. Med. Sci. 17 (1) (2018) 42–49.
[24] H. Kim, S.H. Choi, J.H. Kim, et al., Gliomas: application of cumulative histogram analysis of normalized cerebral blood volume on 3 T MRI to tumor grading, PLoS One 8 (5) (2013) e63462.
[25] K. Skogen, A. Schulz, J.B. Dormagen, et al., Diagnostic performance of texture analysis on MRI in grading cerebral gliomas, Eur. J. Radiol. 85 (4) (2016) 824–829.
[26] T.P. Coroller, W.L. Bi, E. Huynh, et al., Radiographic prediction of meningioma grade by semantic and radiomic features, PLoS One 12 (11) (2017) e0187908.
[27] G.A. Gihr, D. Horvath-Rizea, P. Kohlhof-Meinecke, et al., Histogram profiling of post-contrast T1-Weighted MRI gives ValuableInsights into tumor biology and enables prediction of GrowthKinetics and prognosis in meningiomas, Transl. Oncol. 11 (4) (2018) 957–961.
[28] S. Buttrick, A.H. Shah, R.J. Komotar, et al., Management of atypical and anaplastic meningiomas, Neurosurg. Clin. N. Am. 27 (2) (2016) 239–247.
[29] P.J. Cimino, Malignant progression to anaplastic meningioma: neuropathology, molecular pathology, and experimental models, Exp. Mol. Pathol. 99 (2) (2015) 354–359.
[30] F. Todua, S. Chedia, Differentiation between benign and malignant meningiomas using diffusion and perfusion MR imaging, Georgian Med. News 206 (2012) 16–22.
[31] A. Azizyan, P. Eboli, D. Drazin, et al., Differentiation of benign angiomatous and microcystic meningiomas with extensive peritumoral edema from high grade meningiomas with aid of diffusion weighted MRI, Biomed Res. Int. 2014 (2014) 650939.
[32] Z. Liu, C. Wang, H. Wang, et al., Clinical characteristics and treatment of angiomatous meningiomas: a report of 27 cases, Int. J. Clin. Exp. Pathol. 6 (4) (2013) 695–702.
[33] Nader Zakhari, Carlos Torres, Mauricio Castillo, et al., Uncommon cranial meningioma: key imaging features on conventional and advanced imaging, Clin. Neuroradiol. 27 (2017) 135–144.